

RAPID THERMAL ANNEALING OF SILICON SOLAR CELL USING INCOHERENT LIGHT SOURCE

Raid A. Ismail, Mouslm F. Jawod, *Suad K. Kalil

School of applied sciences, University of Technology. Baghdad- Iraq

*Department of Physics, College of Education for Women, University of Baghdad. Baghdad- Iraq

Abstract

The rapid thermal annealing (RTA) of single crystal silicon solar cell using the radiation from a halogen lamp has been demonstrated. The electrical properties under dark and illumination conditions followed by RTA are presented. The maximum conversion efficiency and filling factor obtained after 1000 °C/ 5 S RTA were 15% and 0.7, respectively.

*

*

% . %

1. Introduction

Much research has been conducted in search of annealing processes which can simultaneously achieve very high electrical activation regions, minimal dopant diffusion, epitaxial regrowth of ion implanted layers, and ion-implanted junctions free from crystal defect for very large scale integrated (VLSI) application [1-4]. This type of control cannot be repeatably demonstrated in classical thermal annealing (furnace annealing). One technology which has received attention is RTA during which the samples are heated with high temperature for a short exposure to an incoherent light source

[5-8]. RTA is a method which uniformly heats and cools sample in seconds. Since the process heats the whole sample, the heating and cooling processes are limited by the thermal mass of the sample and the heat flow mechanism operating on the sample [9].

In this work, we report RTA results for silicon solar cell. The main characteristics of solar cell as function of annealing temperature and annealing time are investigated.

2. Background

The rapid isothermal processing (RIP) cycle consists of three regions a) heating b) quasiequilibrium c) cooling. Supposing that the specimen

is uniformly exposed, the equation to be solved for the heat flow produced by the incoherent source is the diffusion equation which is given by [1].

$$\rho C_p(T) \frac{\partial T}{\partial t} = \nabla(K(T)\nabla T) + p(\gamma, T, t) \dots\dots(1)$$

Where

- ρ: density of processed material
- C_p: specific heat
- K: thermal conductivity
- P: absorbed power distribution for radiation source.

The above equation is non-linear and can be solved subject to certain boundary conditions. In the case of one-dimensional treatment equation (1) is reduced to

$$\rho C_p(T) \frac{\partial T(x,t)}{\partial t} = \frac{\partial}{\partial x} (K(T) \frac{\partial T(x,t)}{\partial x}) + p(x, T, t) \dots\dots(2)$$

The power terms consist of radiation power absorbed, emitted, and lost by conversion or conduction.

A simple approach to solving equation (2) for the temperature of a silicon wafer during power absorption is described by Seidal et al [2] equation (2) is then reduced to

$$\rho C_p(T) \frac{\partial T}{\partial t} = p_a - p_i \dots\dots(3)$$

Where:

- P_a is the instantaneous power absorbed
- and P_i is power lost by radiation or convection.

. Experimental details

Samples used in this work were ± 0.5 μm thick, (100)-oriented wafer of phosphorus doped CZ silicon crystal with electrical resistivity of 1 Ω.cm. The samples rinsed in HF to remove native oxide. After etching process the samples were doped with boron with junction depth about 0.5 μm to make p + n solar cell. After doping the samples transferred directly to RTA system. Rapid annealing is carried out using Heat pulse tungsten halogen lamp for different durations (5 - 15) sec at different temperature (400 - 600) °C of one-sided illumination (p-type side). The samples are positioned inside evacuated quartz ampoule with vacuum pressure 10⁻³ Torr.

The schematic of set-up used in this experiment is shown in Figure 1. The temperature on the wafer was monitored by k-type thermocouple attached to the n-side of the wafer. The precision of the temperature measurement from run to another was about ± 1%. Figure 2 shows the temperature- time curve. The ohmic contact to back surface achieved by evaporation of high purity Al by thermal resistive technique. The collection grid was prepared by evaporation of 100 Å of Al through the mask. Finally, an antireflection (AR) coating of 100 Å of TiO₂ was deposited on cells by electron gun system. The main characteristics of solar cells were measured at R.T in a simulator using halogen lamp, which produces AM1, spectrum, the lamp adjusted to power density of 100 mW/cm².

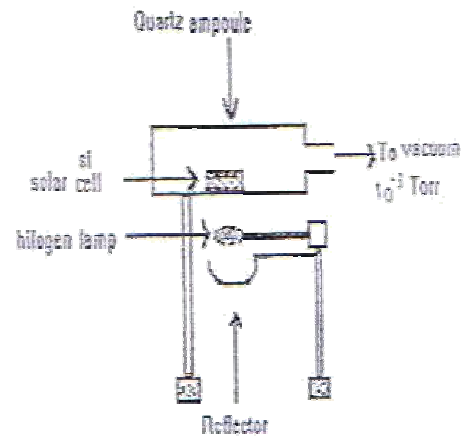


Figure 1: Schematic diagram of experimental set-up

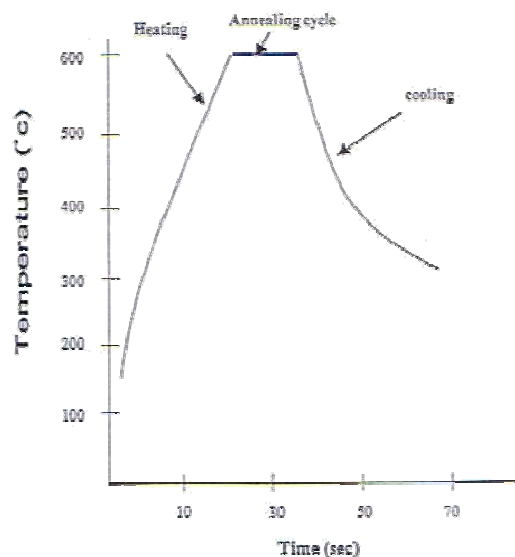


Figure 1: Temperature–Time Curve

Results and Discussion

The forward and reverse I-V characteristics of unannealed p+n cell under dark condition is shown in Figure 2. It is obvious from the figure that the diode shows poor I-V characteristic with high value of recombination current, in addition to that the effect of series resistance exhibited a curvature at $V_a > 0.5$.

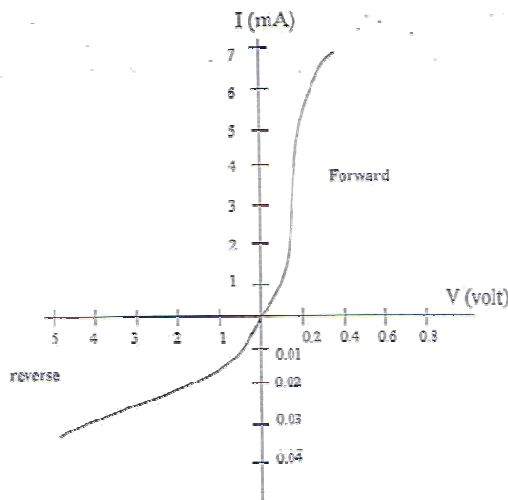


Figure 3: I-V characteristics of unannealed cells

Figure 3 shows the I-V curves of cells treated with different conditions. It is clear from the Figure 3 that the forward current of the diodes follows the ideal diode equation

$$I = I_o (e^{qv_a/nKT} - 1) \dots \dots (4)$$

Where

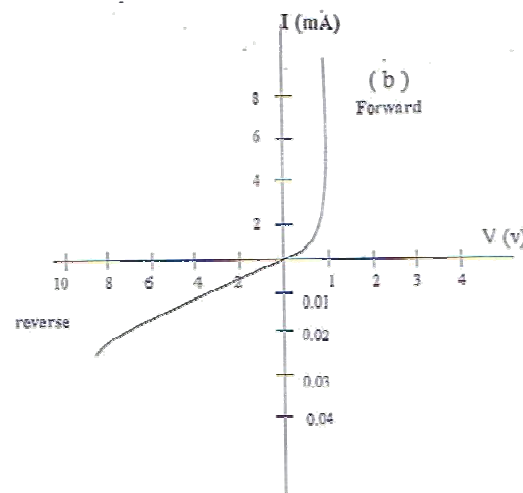
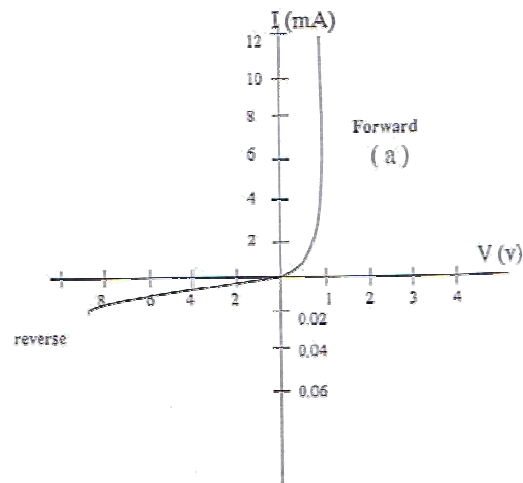
I_o : saturation current

n: ideality factor

For voltage higher than 0.5 V the ideality factor was about 1.5 for all processed diodes, as well as the leakage current at all treated cells is reduced after RTA, indicative of current flow dominated by diffusion, on the other hand there is no observed effect of series resistance after RTA. This implies that the structural defects are removed completely and the boron dopants are fully activated after RTA. The results obtained of solar cell before and after RTA are summarized in table 1.

A detailed analysis of these results demonstrated that the open-circuit voltage V_{oc} (0.5 - 0.6 V) for annealed samples calculated from I-V characteristics under illumination condition are somewhat high compared to those obtained for unannealed cells as shown in Figure 4 this is may be due to the following reasons [10-12]:

- (i). decreasing the defect densities.
- (ii). crystallization recovery.
- (iii). near complete activation of dopants.
- (iv). increasing the diffusion length of the carriers



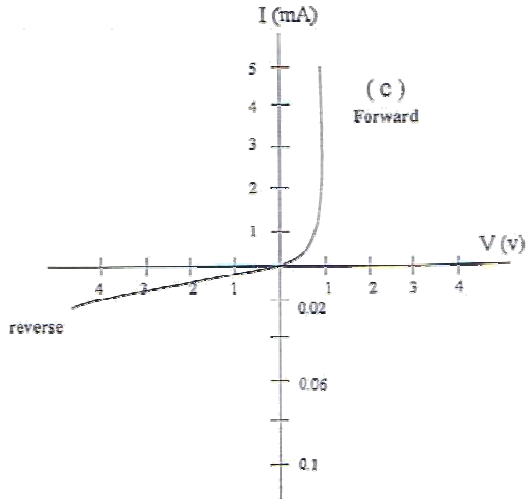


Figure 4: I-V characteristics of annealed cells processed with different conditions (a) 100°C/2 sec, (b) 400°C/2 sec, (c) 600°C/2 sec

Table 1: Solar cell parameters obtained under AMI illumination condition

Annealing Temperature (°C)	Annealing Time (sec)	η %	F.F
Unannealed		10	0.69
100	20	10.5	0.67
200	20	10.7	0.67
300	20	11	0.71
400	20	11.3	0.71
500	20	11.7	0.73
600	20	13	0.65
600	2	10.7	0.69
600	7	11.1	0.69
600	12	11.7	0.71
600	17	12.3	0.73

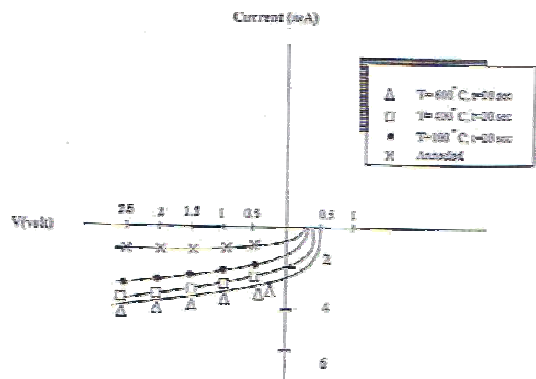


Figure 5: I-V characteristics under illumination condition for cells treated with different annealing temperatures

It is clear from table that the maximum conversion efficiency was for cells annealed rapidly with 600°C/ sec, this result could be

attributed to increasing the concentration of substitutional boron dopant, as well as the extended defects are removed after annealing at 600°C.

No pronounced change of solar cell main parameters has been found after more than six months, which give an indication that the annealed cells have good stability. RTA of solar cell at temperature > 600°C are in progress.

Conclusions

In this paper we studied the annealing of single crystal silicon solar cell by means of rapid thermal annealing (RTA). The effect of annealing conditions on solar cell main parameters is demonstrated. Electrical data under dark and illumination conditions indicate that the annealed layers have highly activated dopants and low concentration of residual defects.

References

1. Narayan, J.; Holland, O.W. and Eby, R.E. *Appl. Phys. Lett.*, 1981, 39, 1037.

2. Singh, R. *J. Appl. Phys.*, 1982, 52, 1037.

3. Susi, E.; Poggi, A.; Fabbri, R. and Merli, M. *Mat. Sci. Eng., B*, 1993, 10, 1037.

4. Gecim, H. S.; Suda, Y.; Tong, B. Y. and Wong, S. K. *solid-state Electronics*, 1994, 35, 1037.

5. Rao, M.V. *Appl. Phys. Lett.*, 1995, 67, 1037.

6. Peter, C. R. *J. Appl. Phys.*, 1996, 79, 1037.

7. Usami, A.; Ando, M.; Tsunekane, M. and Wada, T. *IEEE Trans. Electron Devices*, 1997, 44, 1037.

8. Yelundur, V.; Rohatgi, A.; Jeong, J.; Hanoka, J. *IEEE tran. on Elec. Dev.*, (1998): 46, 1037.

9. Yano, K.; Nandwana, V.; Poudyal, N.; Rong, C. *J. Liu, J. Appl. phys.*, 1999, 86, 1037.

10. Sedel, T.; Knoell, R.; Poli, G.; Schwartz, B.; and Chu, P. *J. Appl. Phys.*, 2000, 88, 1037.

11. Moslehi, M. M.; Chapman, R. A.; Wong, M.; Paranjee, A.; Najem, H. N. and Davis, C. J. *IEEE Trans. Electron Devices*, (): .
12. Lee, J. L.; Wei, L.; Tanigawa, S. and Lee, J. Y. . *IEEE Trans. Electron Devices*, : .
13. Sturm, J. C. and Reaves, C. M. . *IEEE Trans. Electron Devices*, : .